

Solvation Statics and Dynamics of Coumarin 153 in Dioxane–Water Solvent Mixtures

Tatiana Molotsky and Dan Huppert*

Raymond and Beverly Sackler Faculty of Exact Sciences, School of Chemistry, Tel Aviv University, Tel Aviv 69978, Israel

Received: March 25, 2003; In Final Form: August 18, 2003

We studied the solvation statics and dynamics of coumarin 153 dye in a dioxane–water binary solvent mixture. The solvation energy of coumarin 153, both in the ground and excited electronic states in dioxane–water mixtures, exhibits a nearly linear solvatochromic shift as a function of the polar solvent mole fraction. Part of the solvation dynamics of the dye in its excited state is rather slow and almost independent of the mixture composition. The slow solvation dynamics arose from the presence of large cosolvent oligomers due to the strong association of the two liquids rather than the dielectric enrichment or specific hydrogen bonding to the dye in these mixtures.

Introduction

The importance of solvents in chemistry is widely discussed in the literature. Solvents alter the pathways of reactions and change the energies of the reactants. This is one of the reasons for research on solvation and solvation dynamics. Solvation statics and dynamics have been extensively studied.^{1–7} Ultra-short laser pulses of picosecond and femtosecond time duration have been used during the last two decades to study solvation processes on a femtosecond–picosecond time scale. In these studies, the solvation dynamics were monitored via the time-dependent spectral shift of the fluorescence band of a probe molecule dissolved in the solvent under study.

Barbara and co-workers,⁸ as well as Maroncelli and co-workers,⁹ studied the solvation dynamics of a probe molecule in binary polar solvent mixtures. The neat liquids are both aprotic solvents, the equilibrium solvation properties of which are sufficiently similar that the occurrence of preferential solvation is not expected in their binary mixtures. Gardecki and Maroncelli⁹ found that the steady-state solvent nuclear reorganization energy in these mixtures is essentially invariant to the composition of these mixtures. Solvation times in the binary mixtures vary, between the pure solvent limits, with the composition of solvent mixtures. The dependence of the characteristic solvation times on composition is related to other dynamic properties, such as solute rotation times and solution viscosity. Furthermore, the dependence of the dynamics on the composition can be described by a linear function of the mole fraction of one of the solvent mixture constituents.

The solvation of probe molecules in mixtures of polar and nonpolar solvents has been investigated.^{10–34} The solvation in polar and nonpolar solvents is distinctly different from that in mixtures of two polar solvents. In neat polar solvents, such as nitriles, water or alcohols, the solvent molecules reorient themselves around the photoexcited molecule. In mixtures of polar and nonpolar solvents, the slow part of the solvation dynamics due to polar solvent–probe interaction arises from translational polar solvent motions. If the concentration of the more polar solvent is greater in the solvation shells of the solute

than in the bulk concentration, the solute is preferentially solvated and the solvatochromic shift of fluorescence or absorption bands deviates from linear dependence. In these systems two processes contribute to the solvation of the excited polar solute: reorientation of polar solvent molecules and translational diffusion of more polar solvent molecules to the molecule probe.

Several theoretical models describing preferential solvation phenomena were developed. Preferential solvation was discussed in detail by Suppan,^{10–13} who introduced the index of preferential solvation, Z . Suppan used a continuum model to describe preferential solvation. Kauffman and co-workers^{16,17} extended Suppan's theory by distinguishing the influence of mixture nonideality from the influence of dielectric enrichment. Recently, Agmon²³ developed the dielectric enrichment model, based on the extension of the Smoluchowski aggregation model. The theory involves many aggregates of a solute surrounded by various compositions of the mixture. The two extreme cases of aggregates are the ones containing either n nonpolar molecules, PS_N^n , or, in the opposite case, n polar solvent molecules in the first solvation shell, PS_p^n . The general case is several polar solvent molecules in the first solvation shell, such as $PS_N^{n-i}S_p^i$, where $i > 1$. The model explains the main aspects of the concentration and time dependence of preferential solvation. We successfully used Agmon's model to explain both the static and dynamic spectroscopic results of a coumarin 153 hexane-propionitrile solution.²⁴

Chandra and Bagchi²⁵ proposed the molecular theory of solvation in a binary mixture. The theory shows that (1) the nonideality of solvation depends strongly on both the molecular size and the magnitude of the dipole moment of the solvent molecules; (2) the continuum model is inaccurate in explaining the solvation dynamics in binary mixtures; (3) the dynamics of solvation in a binary liquid is nonexponential; (4) the dependence of $\langle \tau \rangle$ on the mole fraction for binary mixtures is nonlinear.

Several experimental studies on preferential solvation have been carried out. Suppan^{10–13} investigated several mixtures and found that some mixtures behave "ideally" (the cyclohexane–tetrahydrofuran system) whereas others show slight (diisopropyl ether–dimethylformamide) or relatively large (n -hexane–

* Corresponding author. Fax/phone: 972-3-6407012. E-mail: huppert@tulip.tau.ac.il.

propionitrile) deviations from linearity. Raju and Costa²⁶ studied the absorption and emission properties of 7-(diethylamino)-coumarin dyes in dioxane–water mixtures. They did not observe dielectric enrichment around the dyes in these mixtures. Rempel and co-workers²¹ measured a time-resolved Stokes shift and the steady-state absorption and fluorescence of coumarin 153 in binary mixtures of alcohols and alkanes at various alcohol concentrations. Depending on the alcohol concentration, the Stokes shift occurs on a time scale ranging from 300 ps to several nanoseconds. They explained their results along the lines of Suppan's theory^{10–13} of preferential solvation with non-specific interaction.

Levinger and co-workers²² studied the solvation dynamics of C153 in an acetonitrile–benzene nonassociating mixture of a dipolar solvent, acetonitrile, and a quadrupolar solvent, benzene. The solvation response observed is sensitive to the mixing of the pure solvents, affecting both the inertial and diffusive components of the solvation response function. Addition of acetonitrile to benzene increases the amplitude of the inertial response. At high benzene mole fractions, the diffusive relaxation reveals a slow component attributed to translational diffusion of the acetonitrile.

Another class of solute–solvent mixture behavior is a specific hydrogen bond with the large probe molecule. Jarzeba and co-workers²⁷ studied the solvation statics of coumarin 153 in toluene–methanol mixtures. For the excited coumarin 153 in toluene–methanol mixtures, strong nonlinearity in the fluorescence solvatochromic shifts is mainly attributed to the formation of a hydrogen bond between the methanol and coumarin 153. We studied the solvation statics and dynamics of coumarin 153 and 102 dyes in hexane–methanol mixtures.²⁸ We analyzed the statics and dynamics of the solvation of coumarin dyes in a hexane–methanol mixture using a model of two distinct solvates. The first solvate is a coumarin dye that is not hydrogen bonded at the carbonyl group. The second solvate has a specific hydrogen bond between the hydroxyl group of the methanol and the carbonyl group of the coumarin dye. The excited-state dynamics are followed by time-resolved emission and the analysis is based on the irreversible diffusion-influenced chemical reaction formalism.

In this study, we further explore the static and dynamics of a polar fluorescent probe molecule in a solvent binary mixture. We measure the absorption, emission, and time-resolved fluorescence spectra of coumarin 153 in dioxane–water solvent mixtures. Coumarin 153 (C153) is a rigid molecule with a single low-lying excited state and simple solvatochromic behavior. The excited-state lifetime, τ_F , of C153 is ~ 5 ns. A relatively large dipole moment of 4.5 D for S_0 indicates that C153 should be strongly solvated in the ground state. The dipole moment of the excited state increases to 11 D. As a result of the increase of the dipole moment of the C153 molecule, the solvation of the S_1 state of C153 should be qualitatively similar to, but larger than, the solvation of the ground state. Dioxane–water solvent mixtures were examined here. The spectral shift of the steady state absorption and emission of coumarin 153 in dioxane–water binary solutions is nearly linear to the composition of these mixtures. In addition, the time-resolved study shows an unusual, slow solvation response of about 180 ps almost independent of the water mole fraction (up to 0.4). Thus, preferential solvation does not occur in these binary mixtures. We attribute the experimental solvation dynamics results to the rotation of large dioxane water aggregates rather than the translational motion of a water molecule toward the first solvation shell. Infrared, nuclear magnetic resonance, Raman

and Rayleigh light scattering studies of 1,4-dioxane–water binary mixture show the existence of relatively large aggregates composed of dioxane–water molecules.

Experimental Section

Time-resolved fluorescence was detected using a time-correlated single-photon-counting (TCSPC) technique. As a sample excitation source, we used a CW mode-locked Nd:YAG-pumped dye laser (Coherent Nd:YAG Antares and a cavity dumped 702 dye laser) that provided a high repetition rate of short pulses (2 ps at full width at half-maximum (fwhm)). The TCSPC detection system is based on a multichannel plate Hamamatsu 3809 photomultiplier and a Tennelec 864 TAC and 454 discriminator. A personal computer was used as a multi-channel analyzer as well as for data storage and processing. The overall instrumental response was about 40 ps (fwhm). Measurements were taken at 10 or 20 ns full scale. The samples were excited at 310 nm (the second harmonic of the Rhodamine 6G dye laser). At this wavelength, a sample is excited to S_2 , the second excited electronic state. The transition dipole moment S_0 – S_2 is perpendicular to S_0 – S_1 . Therefore, a polarizer set at an angle complementary to the “magic angle” was placed in the fluorescence collection system.

Absorption spectra were acquired with a Perkin-Elmer model 551S UV–vis spectrometer. Steady-state fluorescence spectra of the samples were recorded on an SLM-Aminco-Bowman 2 luminescence spectrometer and corrected according to manufacturer specifications.

Coumarin 153 was purchased from Exciton and used without further purification. Dioxane was purchased from Aldrich and used without further purification. All experiments were performed at room temperature (23 ± 2 °C).

Data Analysis of Static Absorption and Emission Spectra

The absorption and emission bands of dioxane–water mixtures are broad and structureless and can be described by a log-normal distribution function.

$$I(\nu) = h \begin{cases} \exp[-\ln(2)\{\ln(1 + \alpha)/\gamma\}^2] & \alpha > -1 \\ 0 & \alpha \leq -1 \end{cases} \quad (1)$$

with

$$\alpha \equiv 2\gamma(\nu - \nu_p)/\Delta$$

fluorescence intensity at frequency (ν), h the peak height, ν_p the peak frequency, γ the asymmetry parameter, and Δ represents the band's width.

Results

Steady-State Absorption and Fluorescence Spectra. Steady-state absorption and emission spectra of coumarin 153 were measured in dioxane–water mixtures at different water concentrations. Figures 1 and 2 show the absorption and emission spectra of coumarin 153 in various dioxane–water mixtures, respectively. The absorption and fluorescence bands of C153 in these mixtures (Figures 1 and 2) do not show any vibrational structure even in neat dioxane. The absorption and emission bands of dioxane–water mixtures were fitted by a log-normal distribution function (see eq 1). The relevant parameters for the analysis of these mixtures are given in Table 1. The absorption and fluorescence bands shift further to the red with increasing concentration of a polar component (water) in the solvent mixtures. The observed red shift of the fluorescence band, due

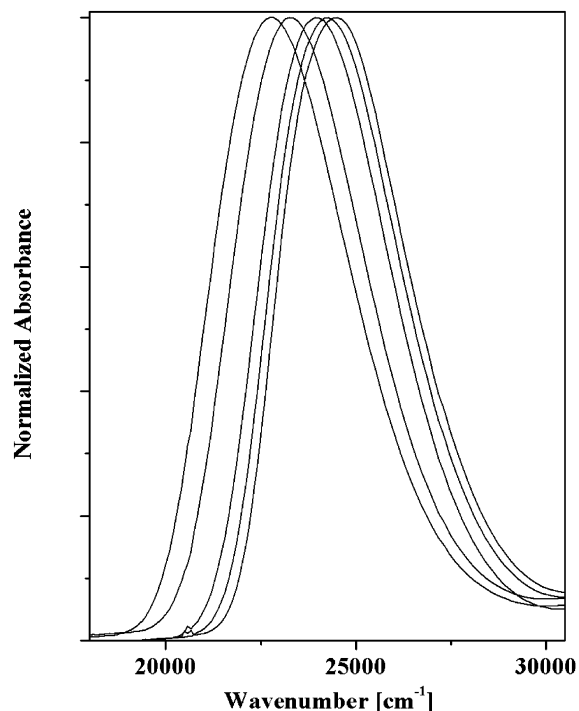


Figure 1. Normalized absorption spectra of coumarin 153 in dioxane–water mixtures as a function of the water mole fraction. Right to left: $x_p = 0, 0.13, 0.34, 0.76,$ and 0.95 .

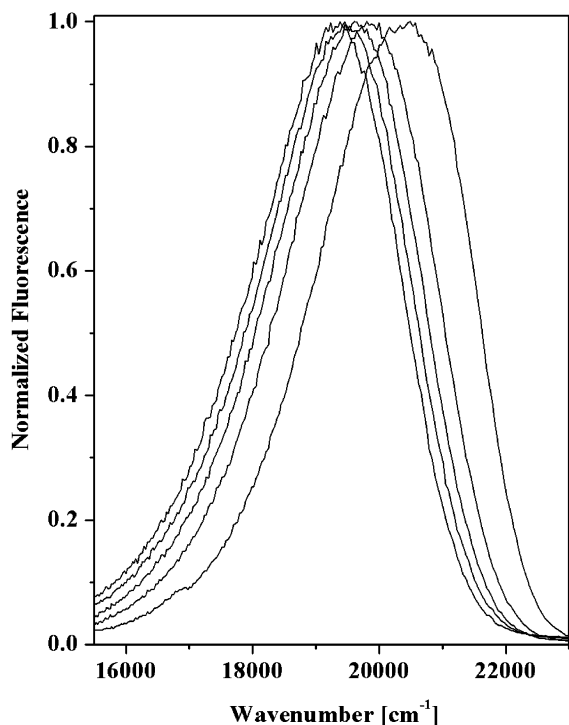


Figure 2. Fluorescence spectra of coumarin 153 in dioxane–water mixtures as a function of the water mole fraction. Right to left: $x_p = 0, 0.13, 0.2, 0.28,$ and 0.34 . Excitation wavelengths are at the absorption maximum.

to increasing water concentrations, is larger than that of the absorption spectra. With increasing water concentration, the bandwidth of absorption and emission spectra increases. Many theories of varying complexity have been advanced to explain the observed changes in the emission energy of a probe in terms of the dielectric properties of the solvent and the ground- and excited-state dipole moments of the probe. The band shift of the emission energy (E_{fl})^{14,15} is related to the excited- and

TABLE 1: Characteristic Parameters for a Single Log-Normal Fit of the Absorption and Emission Band of C153 in Dioxane/H₂O Mixtures^a

x_{H_2O}	absorption			emission		
	γ	ν_p (cm^{-1})	Δ (cm^{-1})	γ	ν_p (cm^{-1})	Δ (cm^{-1})
0	0.37	24400	3825	-0.27	20400	2800
0.13	0.38	24200	3850	-0.27	19850	2800
0.2	0.37	24100	3900	-0.28	19600	2800
0.28	0.35	24000	3900	-0.29	19450	2825
0.34	0.34	23950	3900	-0.30	19300	2825
0.4	0.33	23900	3900	-0.30	19250	2825
0.54	0.33	23650	3925	-0.30	18600	3250
0.67	0.33	23450	3950	-0.31	18400	3200
0.76	0.33	23250	3970	-0.31	18300	3200
0.83	0.32	23100	3975	-0.31	18200	3200
0.88	0.32	22950	3975	-0.31	18050	3200
0.95	0.32	22750	4100	-0.31	17850	3200
0.98	0.32	22750	4170	-0.33	17800	3225

^a x_{H_2O} are the water mole fractions, γ the asymmetry of the peak, ν_p the location of the peak maximum, and Δ the peak width.

ground-state dipole moments (μ_e and μ_g) through the static dielectric constant (ϵ) of the solvent by

$$E_{fl} = [\mu_e(\mu_g - \mu_e)/a^3]F(\epsilon) \quad (2)$$

The polarity of a solvent is defined as a function F of the dielectric constant ϵ . Onsager's function is given by

$$F(\epsilon) = \frac{2(\epsilon - 1)}{2\epsilon + 1} \quad (3)$$

The polarity of an "ideal" mixture of two solvents composed of nonpolar, N , and polar, P , solvents whose dielectric constants are ϵ_N and ϵ_P respectively, is a simple linear combination according to their mole fraction x_N and x_P

$$F_{linear,bulk} = x_N F_N + x_P F_P \quad (4)$$

The real experimental dielectric constant, ϵ ,³⁵ of dioxane–water mixtures deviates from that of an "ideal" mixture and has been fitted to the following empirical composition dependences:

$$\epsilon = 2.34255 - 20.24172x_p + 186.04527x_p^2 - 362.27023x_p^3 + 271.95435x_p^4$$

Figure 3 shows the polarity function $F(\epsilon)$ as a function of x_p . The dioxane–water mixtures show nonideal behavior over the entire concentration range. Such behavior was expected due to the association properties of dioxane and water molecules and the self-association properties of dioxane and water molecules.

When the Onsager polarity of the two cosolvents is very different, their distribution next to a dipolar solute is then not the same as the undisturbed bulk. If x_N and x_P are the mole fractions of the bulk, then next to the solute, the mole fractions become y_N and y_P . The mole ratios $X = x_N/x_P$ and $Y = y_N/y_P$ are then related by $Y = Xe^Z$. A single shell approximation to Z is given by Suppan¹⁰

$$Z = \frac{1}{4\pi\epsilon_0} \frac{CM\mu^2\Delta F_{N,P}}{2\delta RT r^6} \quad (5)$$

$$\Delta F_{N,P} = F_P - F_N \quad (6)$$

where $\Delta F_{N,P}$ is the difference of the Onsager's functions of pure polar and pure nonpolar solvents, the solvent dipoles, set at a

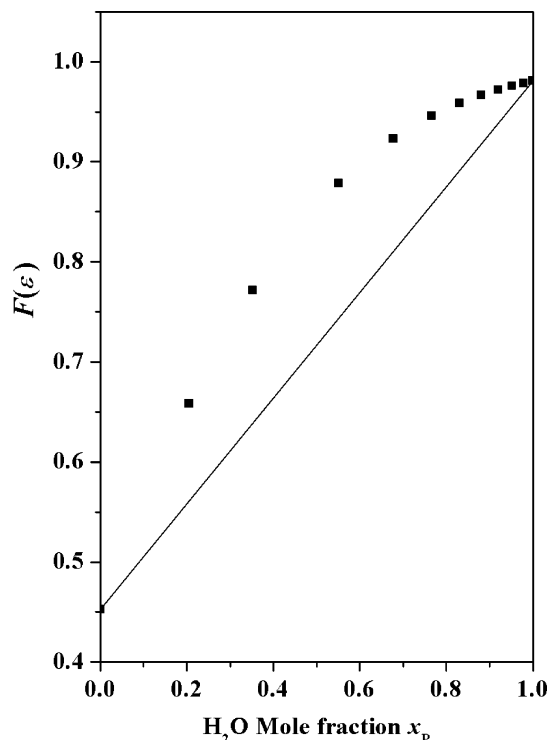


Figure 3. Onsager polarity function, $F(\epsilon)$, plotted as a function of the mole fraction of water solvents. Dioxane–water mixtures are shown as squares. The calculated ideal mixture (eq 4) is shown as a solid line.

fixed distance from the solute dipole center, C , in a numerical factor in the order of unity, μ the solute dipole moment, M is the mean molar weight of the polar and nonpolar solvents, R is the gas constant, T is the temperature, and δ is the mean density of the two solvent components.

Dielectric “nonideality” of a binary solvent system refers to the deviation of the Onsager reaction field function from linearity in the polar mole fraction of the solvent mixture. A dipolar fluorophore, dissolved in an ideal dielectric mixture, exhibits a solvatochromic shift that is linear to the solvent polar mole fraction in its solvation sphere. As a result, the “local composition” can easily be determined from the peak shift. Kauffman and co workers^{16,17} have identified conditions under which the linear approximation is justified and find that, for most cases of practical importance, the linear approximation will not provide accurate estimates of the local solvent composition from solvatochromic studies. Similarly, solvatochromic shifts can only be accurately predicted from theoretical local compositions if dielectric nonideality is taken into account. The Z value, due to preferential solvation, Z_{ps} , is related to experimental spectral shift data by employing the so-called “nonlinearity ratio”, ρ_{exp} . This quantity can be calculated from measured quantities using the expression

$$\rho_{exp} = \frac{2 \int_0^1 (E_{exp} - E_{linear,bulk}) dx_p}{\Delta E_{N,P}} \quad (7)$$

where E_{exp} is the experimental peak energy of the fluorophore at bulk polar mole fraction x_p and $E_{linear,bulk} = x_p E_P + x_N E_N$ is the calculated peak energy of the fluorophore, assuming that it is dissolved in an ideal binary mixture at bulk polar mole fraction x_p and $\Delta E_{N,P}$ is the difference in peak energies in the neat polar and nonpolar solvents. Two factors contribute to the difference between E_{exp} and $E_{linear,bulk}$, preferential solvation and dielectric

nonideality. The experimental nonlinearity ratio, ρ_{exp} , can be expressed as the following sum:

$$\rho_{exp} = \rho_{ps} + \rho_{ni} \quad (8)$$

in which ρ_{ps} and ρ_{ni} are the contributions of preferential solvation and dielectric nonideality to the experimental nonlinearity ratio, respectively. The dielectric nonideality contribution, ρ_{ni} , can be calculated from experimental dielectric constant measurements using the expression

$$\rho_{ni} = \frac{2 \int_0^1 (E_{exp} - E_{linear,bulk}) dx_p}{\Delta F_{N,P}} \quad (9)$$

where $\Delta E_{N,P}$ is the difference of the Onsager’s functions of pure polar and pure nonpolar solvents (see eq 6) and F_{exp} is the Onsager’s function that we calculated, using eq 3, from the dielectric constant, ϵ , measured for these mixtures. $F_{linear,bulk}$ is calculated for an ideal dielectric mixture from eq 4. Kauffman and co-workers^{16,17} have shown that when ρ_{ps} is less than 1, the relationship between ρ_{ps} and Z_{ps} is well approximated by the expression

$$\rho_{ps} = 0.31 Z_{ps} \quad (10)$$

Using eqs 3, 4, 6, and 9, we calculated the dielectric nonideality contribution, ρ_{ni} , for the dioxane–water mixture to be $\rho_{ni} = 0.28$. Using eq 7 and the data in Table 1, we obtain the nonlinearity ratios $\rho_{exp} = -0.08$ and $+0.12$ for the ground and excited states, respectively. Using eqs 8 and 10 and the above values of ρ_{exp} and ρ_{ni} , we find negative values for Z_{ps} , i.e., -1.17 and -0.51 for the ground and excited states, respectively. In contrast to these findings in mixtures of hexane–propionitrile²⁴ and other similar nonassociative solvent mixtures, Z_{ps} is positive. We shall discuss that issue in the next section.

The solvatochromic shift of the absorption and fluorescence bands of C153 in dioxane–water mixtures as a function of the mole fraction of the more polar solvent is plotted in Figure 4. The data presented in Figure 4 show that the red shifts of the absorption and fluorescence bands of C153 in dioxane–water mixtures are a linear function of the polar solvent mole fraction. To analyze solvatochromic shifts, it is convenient to employ the reaction field factor, $F(\epsilon)$, as the solvent polarity scale. The dielectric continuum theory predicts that solvatochromic shifts of the absorption and fluorescence spectra for a molecule in solvents of different polarity should be proportional to $F(\epsilon)$.³⁶ Figure 5 shows plots of solvatochromic shifts of C153 in the dioxane–water binary mixtures as a function of $F(\epsilon)$. As seen in Figure 5 the linear plot holds up to approximately $F(\epsilon) = 0.85$, which corresponds to about $x_p = 0.55$ but does not hold for water rich mixtures where $F(\epsilon) > 0.85$. Our time-resolved study was limited to solutions of dioxane–water with relatively small water concentrations. The largest water concentration was $x_p = 0.4$.

Anomaly of Dioxane. Suppan,¹¹ Gustavson,⁴ and Maroncelli³⁶ pointed out that several neat solvents deviate strongly from the simple linear relation between the absorption and emission solvatochromic shift and the probe dipole–solvent interaction. 1,4-Dioxane, which should be nonpolar according to its static dielectric constant $\epsilon = 2.2$, appears almost invariably “pseudopolar” with solvatochromic shifts similar to that of cyclic ethers, like THF, $\pi^* = 0.55$.³⁷ Hydrogen bonding by dioxane itself is small on the Kamlet–Taft scale, $\alpha = 0$ and $\beta = 0.31$.³⁸ The physical properties of dioxane are, in many respects, similar to those of water. For example, their boiling points are within

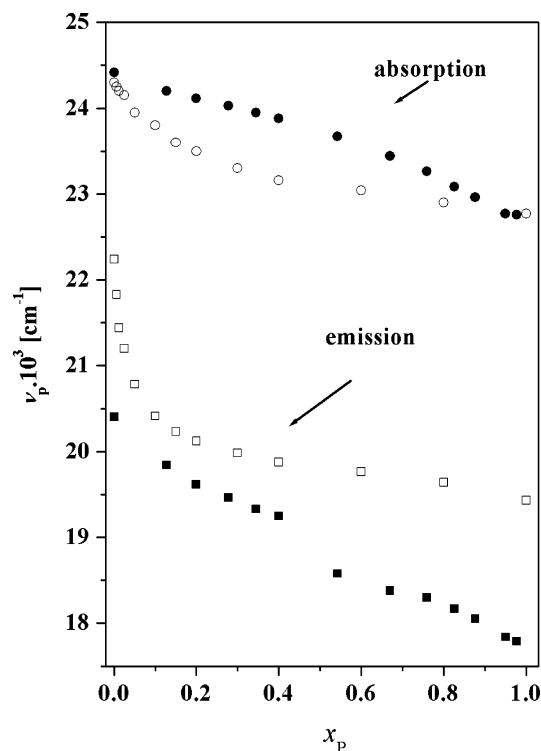


Figure 4. Peak of the absorption and emission spectra of coumarin 153 in a binary solvent mixture as a function of the polar solvent mole fraction: dioxane–water (filled symbols); hexane–propionitrile (open symbols).

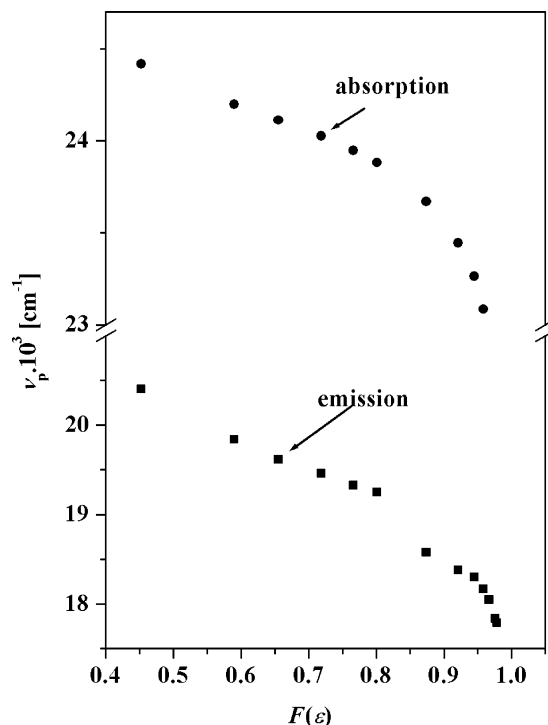


Figure 5. Normalized shift of the maxima of the steady-state absorption and fluorescence spectra of coumarin 153 in dioxane–water mixtures as a function of the Onsager polarity function, $F(\epsilon)$.

1.5°, their freezing points are within 12°, and their heats of vaporization, which are high, are within 2 kcal/mol of each other. They mix in all proportions and provide an opportunity for studying the molecular interactions in these systems. Neat water is a polar liquid with $\pi^* = 1.09$ or $E_N^T = 1.0$ ³⁹ and a high dielectric constant, $\epsilon = 78$. Gustavson and co-workers⁴ and

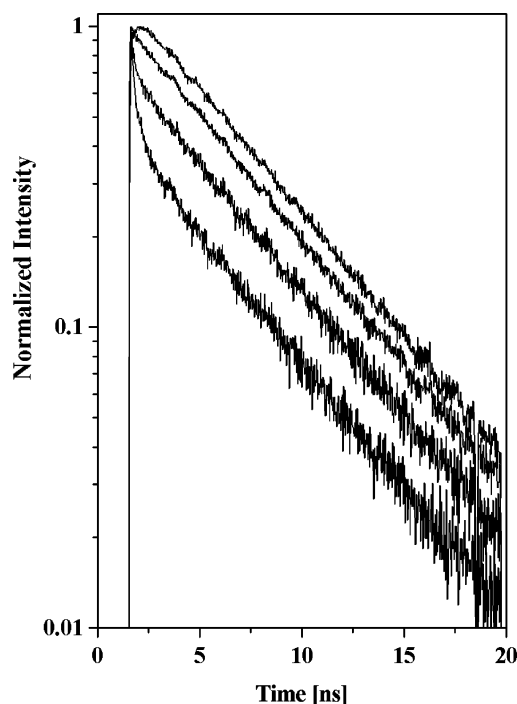


Figure 6. Time-resolved luminescence of C153 in a $x_p = 0.3$ dioxane–water mixture at selected wavelengths. Top to bottom: 570, 510, 490, and 470 nm.

Maroncelli and co-workers³⁶ pointed out that coumarin 153 in neat dioxane exhibits a large Stokes shift even though it is considered a nondipolar solvent. Maroncelli³⁶ explains the large shift by the presence of two polar groups, $\text{CH}_2\text{--O--CH}_2$, in dioxane. One expects the local bond polarities of the $\text{CH}_2\text{--O--CH}_2$ groups in dioxane and THF ($\pi^* = 0.55$) to be similar. The main difference between these two solvents is that, whereas the presence of a single such group in tetrahydrofuran leads to an appreciable dipole moment (1.75 D), the two groups in dioxane oppose each other in such a way that they result in a net zero dipole moment but exhibit a large quadrupole moment in a certain molecular configuration (boat).¹¹ This difference between dioxane and THF leads to vastly different values of their dielectric function, $F(\epsilon, n)$. Despite this difference, the nuclear reorganization energies, measured by the C153 probe, are nearly identical.

Time-Resolved Emission of C153 in Dioxane–Water Mixtures. Figure 6 displays the time-resolved fluorescence data for C153 in $x_p = 0.3$ dioxane–water mixtures measured at various wavelengths. In the dioxane–water mixtures, the fluorescence decay of C153 is dependent on the wavelength detected. The decays at the red end of the fluorescence spectrum are significantly different from those at the blue end of the fluorescence spectrum; the fluorescence decays at the red end exhibit distinct growth, whereas those at the blue end exhibit fast decay. Such wavelength-dependent behavior of the fluorescence decay indicates that the fluorescence of C153 presents a time-dependent Stokes shift (TDFSS) in these mixtures. Also, the wavelength dependence of the decays in the dioxane–water mixtures indicates that the solvation dynamics have slowed and are hence detected in our picosecond setup (time resolution of ~ 20 ps). The observed decay is nonexponential. Time-resolved spectra were constructed and analyzed by a procedure given by Maroncelli and co-workers.¹ Only the long components were accurately time-resolved in this study. The time-resolved emission data collected at 10 nm intervals were analyzed using a convoluted procedure involving the system IRF and a sum of

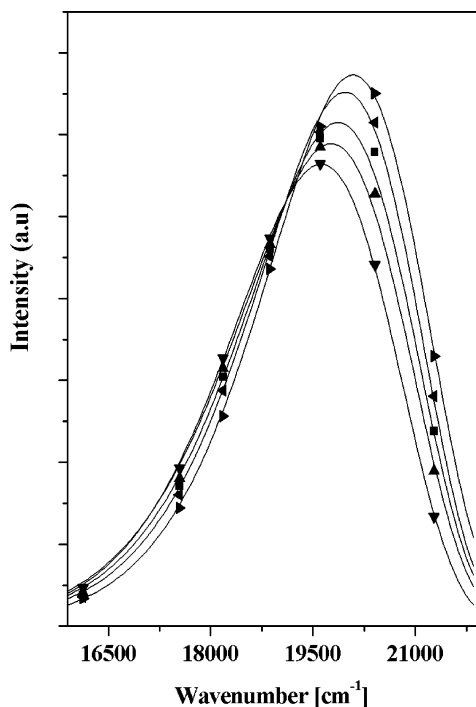


Figure 7. Time-resolved emission spectra of C153 in $x_p = 0.2$ dioxane–water mixtures at various times: 10 (right-pointing triangle); 50 (left-pointing triangle); 100 (■); 200 (▲); and 1000 (▼) ps. Solid lines are computer fits.

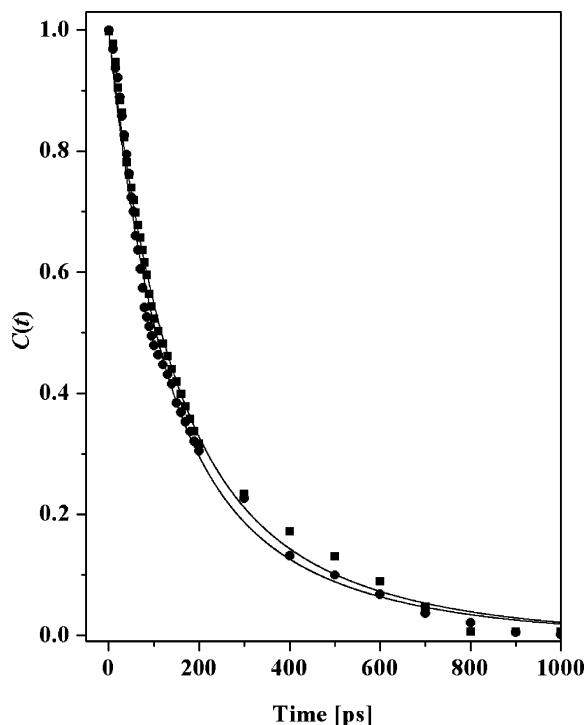


Figure 8. Normalized solvation response function, $C(t)$, of coumarin 153 in dioxane–water mixtures at different water mole fractions. Top to bottom: $x_p = 0.2$ (square) and 0.4 (circle). Solid lines are the biexponential fit to the experimental data.

exponentials. We constructed time dependent spectra, which were fitted to a log-normal function. From the spectral shift of the fluorescence band maximum of coumarin 153 dioxane–water, we constructed the solvation correlation function. Typical time-resolved fluorescence spectra of C153 in a $x_p = 0.2$ dioxane–water mixture are illustrated in Figure 7. Figure 8 shows the solvation correlation function as a function of time

TABLE 2: Relevant Parameters for Time-Resolved Measurements of Dioxane–Water Mixtures and Propionitrile–Hexane Mixtures^a

$x_{\text{H}_2\text{O}}$	$C(t)$ fitting parameters ^b				$\langle \tau \rangle^c$ (ps)	$\Delta\nu^d$ (cm^{-1})	x_{pn}^e	$\langle \tau \rangle^f$ (ps)	$\Delta\nu^g$ (cm^{-1})
	a_1	τ_1 (ps)	a_2	τ_2 (ps)					
0.13	1	160			160	350	0.025	490	1000
0.2	0.58	110	0.42	330	210	500	0.05	370	1100
0.28	0.3	70	0.7	320	240	500	0.1	250	1450
0.4	0.62	100	0.38	330	190	650			

^a The estimated error in the determination of the solvation time τ_1 , τ_2 is $\pm 15\%$, and for $\langle \tau \rangle$, it is $\pm 10\%$. ^b Biexponential fit to the experimental data. ^c Average solvation time ($\langle \tau \rangle$). ^d Spectral shift ($\Delta\nu$). ^e x_{pn} are the propionitrile mole fractions. ^f Average solvation time ($\langle \tau \rangle$) for propionitrile–hexane mixtures.²⁴ ^g Spectral shift ($\Delta\nu$) for propionitrile–hexane mixtures.²⁴

for various compositions of the dioxane–water mixtures. The function $C(t)$ is nonexponential and could be reasonably fitted by two exponentials. The relevant parameters are given in Table 2. The solvation response of coumarin 153 in neat dioxane cannot be observed in the time-resolved emission spectra. The time-resolved emission of coumarin 153 in binary mixtures shows a slow component of about 180 ps. The average relaxation time is almost invariant to the polar solvent concentration.

Discussion

In this study, we measured the solvation energetics and dynamics of coumarin 153 in dioxane–water solutions. Given the large difference between the polarity of water ($\epsilon = 78$ and $\pi^* = 1.09$) and 1,4-dioxane and the large excited-state dipole moment of C153, one might expect preferential solvation of the C153 by water. The main findings of this work are that (a) the band shifts of both the absorption and emission bands are nearly linear to the water mole fraction or the Onsager dielectric function, $F(\epsilon, n)$, up to about $F(\epsilon, n) \sim 0.8$ and (b) the slow component of the solvation dynamics, which is about one-third of the emission spectral shift of C153 in dioxane water mixtures of water mole fraction up to about $x_p = 0.3$, is rather slow and almost independent of solvent composition. The results indicate that dielectric enrichment does not affect the solvation properties.

Gustavsson and co-workers⁴ and Maroncelli and co-workers³⁶ pointed out that coumarin 153 in neat dioxane exhibits a large Stokes shift even though it is considered a nondipolar solvent. Maroncelli explains the large spectral shift of probe molecules in dioxane by a large quadrupole moment arising from the presence of two polar groups, $\text{CH}_2\text{—O—CH}_2$, in dioxane.

Steady-state absorption and fluorescence spectra of C153 in dioxane–water mixtures (see Figures 1 and 2) show red shifts with the addition of water to dioxane. Though both the absorption and emission spectra of coumarin 153 in nonpolar solvents such as hexane and cyclohexane show a clearly resolved vibrational structure, in neat dioxane both spectra are structureless and strongly red shifted with respect to hexane. The large changes in the spectra are mainly attributed to the dipole–quadrupole interaction. The absorption and emission spectral widths also increase when small amounts of water are added to dioxane (see Table 1). Preferential solvation has been investigated through nonideality of absorption and fluorescence spectra.¹⁸ Figure 4 shows the maximum of the absorption and emission bands of C153 in a dioxane–water mixture as a function of the water mole fraction. For comparison, we added the absorption and emission of C153 in hexane–propionitrile mixtures taken from ref 24. As clearly seen in Figure 4, the

band position at the maximum, of both the absorption and emission of C153 in the hexane–propionitrile solution up to $x_P = 0.4$, strongly deviates from linear dependence. In these mixtures, a dielectric enrichment process occurs and $Z_{PS} \sim 1$. The linear dependence of the absorption and fluorescence maxima versus the mole fraction of the dioxane–water mixture up to $x_P \sim 0.5$ suggests that only minor deviations from ideality occur in these mixtures and hence does not indicate that water preferentially solvates C153. C153 dissolves well in polar solvents including monols but does not dissolve in water whereas dioxane and water strongly associate with each other to form oligomers. This fact might partially explain why preferential solvation does not take place in these mixtures. Suppan^{10–12} and Zurawsky and Scarlata^{14,15} showed that non-linearity of the fluorescence spectra as a function of x_P incorrectly predicted preferential solvation and suggested that the continuum reaction field (F) based on the actual experimental static dielectric constant, ϵ , of the mixtures provides a better scale of the spectroscopic measurements. We used this suggestion to study the band position of the absorption and fluorescence spectra as a function of $F(\epsilon)$ (see Figure 5). The dielectric enrichment model predicts deviation from ideal behavior when both μ and $\Delta f(\epsilon)$ are large. Coumarin 153 exhibits a dipole of 4.5 and 11 D in the ground and excited states, respectively, and for water, $\epsilon = 78$ compares with $\epsilon = 2.2$ for dioxane. Thus, the emission band shift of coumarin 153 in the dioxane–water mixture should show a marked deviation from an ideal solution due to the large dipole change between the ground and excited states and the large change in $\Delta f(\epsilon)$. Using eqs 5 and 6 and the relevant parameters for dioxane–water mixtures, $M = 53$ g/mol, $\delta = 1.02$ g/cm³, $\Delta\mu = 6.5$ D (the dipole change upon excitation), and $r = 5.2$ Å leads to $Z \sim 1.4$. If the preferential solvation model is operative then, for $Z = 1.4$, we expect that significant dielectric enrichment will occur upon excitation of coumarin 153. The fluorescence band shift of coumarin 153 as a function of the mole fraction of water should deviate considerably from a linear behavior, which is not the case (as shown in Figure 4). The dioxane–water mixtures show nonideal bulk dielectric behavior over the whole concentration range (see Figure 3). Such behavior was expected due to the association and self-association properties of dioxane and water molecules. In these cases, we observe a substantial influence of dielectric nonideality on possibly solvent–solute interactions. Thus, we separated the influence of mixture nonideality from the influence of preferential solvation using the procedure proposed by Kaufmann and co-workers.^{16,17} Using eq 7, we obtain very small nonlinearity ratios of $\rho_{\text{exp}} = -0.08$ and $+0.12$ from our spectroscopic absorption and emission measurements, respectively. Application of eq 9 to the calculation of nonlinearity resulting from bulk solvent nonideality, ρ_{ni} , using Onsager functions, determined from experimental dielectric constant values, gives $\rho_{\text{ni}} = 0.28$. $\rho_{\text{ni}} = 0.28$ should cause relatively large nonlinear solvatochromic shifts in the plot of both the absorption and fluorescence band positions of C153 as a function of x_P in rich dioxane–water mixtures. But, as seen in Figures 4 and 5, up to $F(\epsilon) \cong 0.85$, the nonlinearity is small. The ρ_{exp} of the dioxane–water solvent mixture is much smaller than that of the bulk dielectric nonideality contribution, ρ_{ni} . In other words, none of the C153 solvates introduce additional nonlinearity to the binary solvent mixture. This implies that there is neither preferential solvation of the dyes nor dielectric enrichment of the medium around the dyes.

Hydrogen Bonding. A plausible explanation of the spectroscopic data of C153 in rich dioxane–water mixtures is the

formation of a hydrogen bond between a water molecule and the coumarin carbonyl. A linear regression fit of the absorption band position of C153 in 15 neat solvents on the Kamlet–Taft scale with the solvent parameters π , α , and β

$$\nu = \nu_0 + p\pi + a\alpha + b\beta \quad (11)$$

yielded²⁸ $\nu_0 = 24.90 \times 10^3$ cm⁻¹, $p = -1780$ cm⁻¹, $a = -540$ cm⁻¹, and $b = 150$ cm⁻¹ with R , the correlation coefficient, being 0.94. A similar linear regression fit of the emission band position of C153 in neat solvents on the Kamlet–Taft scale with the solvent parameters π , α , and β

$$\nu^* = \nu_0^* + p^*\pi + a^*\alpha + b^*\beta \quad (12)$$

yielded²⁸ $\nu_0^* = 21.83 \times 10^3$ cm⁻¹, $p^* = -2620$ cm⁻¹, $a^* = -860$ cm⁻¹, and $b^* = -680$ cm⁻¹ with $R = 0.9$. Using Maroncelli's⁴⁰ data for the emission band position of C102, we found $\nu_0^* = 23.58 \times 10^3$ cm⁻¹, $p^* = -3200$ cm⁻¹, $a^* = -1980$ cm⁻¹, and $b^* = 1060$ cm⁻¹ with $R = 0.97$. From these correlations we concluded that the solvatochromic spectral shifts of C153 due to hydrogen bonding of water to C153 are relatively small (small a and b values in the Kamlet–Taft correlation function) compared with the polar contribution, denoted as p and p^* in eqs 11 and 12. C102 exhibits much stronger shifts, which were attributed to hydrogen bond accepting and donating properties.²⁸

To exclude the idea that the solvation dynamics arise from a hydrogen bonding process of water with excited C153, we used a site-specific hydrogen bonding model that we previously used successfully to analyze the time-resolved fluorescence data and extract the solvation dynamics of coumarin in the hexane–methanol mixture.²⁸ We used a model of two distinct solvates, described in detail in refs 41 and 42, to check the experimental data obtained for C153 in dioxane–water mixtures. We assumed that the first solvate is a coumarin dye in which a water molecule in the first solvation shell is not hydrogen bonded at the carbonyl group. The second solvate has a specific hydrogen bond between the hydroxyl group of the water molecule and the carbonyl group of the coumarin dye. In the excited state, the coumarin dye has a stronger hydrogen bond and hence the time-resolved emission spectra fit simple A → B kinetics. The model was successfully applied to coumarin 153 dye in electrolyte solutions of ethyl acetate and butyl acetate,^{41,42} as well as MeOH–hexane mixtures.²⁸ We found that the two solvate models failed to describe the experimental spectra for C153 in dioxane–water mixtures.

Comparison with Other Studies. We wish to compare our finding of the spectral shifts of C153 in dioxane–water mixtures with other similar studies. Durocher and co-workers³⁰ studied the static and dynamic spectroscopic properties of 2-(*p*-(dimethylamino)phenyl)-3,3-dimethyl-3*H*-indole in dioxane–water mixtures. In contrast to our conclusion, they explained the obtained results by hydrogen bonding between a water molecule and molecule 2-(*p*-(dimethylamino)phenyl)-3,3-dimethyl-3*H*-indole. Andrade and Costa³¹ studied the spectroscopic behavior of Piroxicam in dioxane–water mixtures. They revealed the existence of an isosbestic point at $\lambda = 290$ nm in the absorption spectra and explained it, similarly to Durocher et al.,³⁰ by the existence of a ground-state complex between the probe and water. On the other hand, Raju and Costa²⁶ studied the absorption and emission properties of 7-(diethylamino)-coumarin dyes in dioxane–water mixtures. Similar to our findings, they could not observe dielectric enrichment around the dyes in these mixtures. These findings are similar to the

current study of coumarin 153 in the same binary solvent mixture but different from the behavior we observed in studying coumarin 153 in hexane–propionitrile.²⁴

Time-Dependent Emission. In this study, we attribute the observed emission relaxation time to the rotational motion of relatively large aggregates composed of dioxane–water molecules. There are two features of the emission time-dependent band shifts that support the slow dioxane–water aggregates solvation hypothesis. First, the relaxation for dioxane–water mixtures reveals a slower component, occurring on the 180 ps time scale, which is absent in either of the pure solvents. Second, the average relaxation time, $\langle\tau\rangle$, is nearly independent of the concentration of added water. The dynamics of the dielectric enrichment model predict that the solvation time depends on the polar solvent mole fraction. Rempel²⁰ found that the solvation correlation function of coumarin 153 in hexane–alcohols depends on the alcohol concentration. In addition, we found that the average relaxation time of coumarin 153 in propionitrile–hexane mixtures (see Table 2) is a function of the polar solvent (propionitrile) concentration. In contrast, we found that the solvation dynamics (see Figure 8) in dioxane–water mixtures is nearly independent of the water concentration. Also, the absorption and emission spectral shift of coumarin 153 in the dioxane–water mixture, as a function of x_p ($x_p = 0$ up to $x_p = 1$) fits a linear dependence. The spectral shift as a function of $F(\epsilon)$ fits a linear dependence only in the dioxane rich mixture, i.e., up to $F(\epsilon) \sim 0.8(x_p = 0.55)$.

In dipolar mixtures³² and mixtures of polar and nonpolar solvents,²¹ researchers have proposed that the translational motion of solvent molecules also contribute to the relaxation. For example, in simulations of ion solvation by binary mixtures, Patey and co-workers showed³² that a translational motion of molecules contributes significantly to solvation dynamics. Studying cresyl violet in binary solvents of different polarity components by transient hole burning spectroscopy, Nishiyama and Okada³³ observed a slow relaxation process for the spectral width. They also explained the results as being due to the translational diffusion of the polar component of solvent molecules. In molecular dynamics simulations of solvation dynamics in acetonitrile/benzene mixtures, Ladanyi and Perng³⁴ observed a strong translational component to the dynamics for benzene rich mixtures. They showed that the slowest component of the solvation dynamics arises from the motion of acetonitrile into the first solvation shell displacing benzene molecules. This suggests that the behavior observed for $\langle\tau\rangle$ in Table 2 does not reflect the contribution to the solvation dynamics of bringing water molecules into the first solvation shell of the C153 molecule.

As mentioned above, we attribute the slow emission relaxation time to the rotational motion of dioxane–water aggregates, rather than the dielectric enrichment dynamics. Infrared^{43,44} and nuclear magnetic resonance⁴⁵ studies of water–dioxane mixtures confirm the existence of such complexes. Also, extensive Raman investigation⁴⁶ revealed a definite concentration dependence of the Raman lines of both components. More recently, the frequency variation of the dielectric constant of water–dioxane mixtures⁴⁷ indicated the presence of two dielectric relaxation mechanisms. The low-frequency dispersion was attributed to molecules in the hydrogen-bonded clusters and the high-frequency dispersion to the overall molecular relaxation of the water molecules, which had at most one hydrogen bond. Rayleigh light scattering of 1,4-dioxane (D)–water (W) binary mixtures have been measured at 25 °C.⁴⁸ For 1,4-dioxane–water they⁴⁸ consider that the local structures of the 1,4-dioxane–

water mixed solvent are determined by dissociation equilibrium, $DW_1 \rightleftharpoons D + W_1$. The local structures can thus be roughly considered as $(DW_1)_q$ and D_n . The slow time-scale associated with the orientation dynamics of large dioxane–water aggregates may be compared with similar findings by Yoshida⁴⁹ et al. They measured the dynamics of a butoxyethanol–water mixture of 0.09 alcohol mole fraction by using a neutron spin–echo (NSE) technique. The diffusion coefficients obtained from the intermediate correlation function are about 10^2 times smaller than those of pure water and alcohol, probably reflecting the dynamics of molecular aggregates formed in the mixture, which has been confirmed by previous small-angle neutron scattering.

Summary

We examined the solvation dynamics of coumarin 153 in dioxane–water mixtures. These mixtures exhibit nonideal dielectric behavior. Solvatochromic shifts of absorption and fluorescence spectra of coumarin 153 in this nonideal system are analyzed as a function of solvent polarity. We applied Suppan's theory of dielectric enrichment and Kaufmann's extension of this theory. We also applied a model of two distinct solvates to C153 dissolved in dioxane–water mixtures. The analysis of the experimental results indicates that C153 does not preferentially solvate and does not hydrogen bond in dioxane–water mixtures. We explain the statics and dynamics of the solvation of coumarin 153 in dioxane–water mixtures as follows: Dioxane is a diether, which interacts strongly with water. The mixture of these two strongly associating solvents forms oligomers composed of dioxane–water molecules. The rotational diffusion of these oligomers is rather slow (on the order of 180 ps) whereas the slowest component of the solvation relaxation of coumarin 153 in neat liquids of each of the mixture constituents is on the order of a few picoseconds. We find that the longer components of the solvation dynamics of coumarin 153 in dioxane–water mixtures at $x_p = 0.3$ contributed about $500 \text{ cm}^{-1} \tau$ to the spectral shift. The average solvation time, $\langle\tau\rangle = 180 \text{ ps}$, is almost independent of the mixture composition. The shorter components of the solvation dynamics, which could not be resolved in our TCSPC system, contribute about $\sim 1000 \text{ cm}^{-1}$. The short components are attributed to the ultrafast rotational motion of monomers of both water and dioxane that occur within a few picoseconds.

Acknowledgment. We thank Dr. Beverly Lewin for her assistance in the preparation of the text. This work was supported by a grant from the James-Franck German-Israel program in laser-matter interaction.

References and Notes

- (1) Horng, M. L.; Gardecki, J.; Papazyan, A.; Maroncelli, M. *J. Phys. Chem.* **1995**, *99*, 17311.
- (2) Barbara, P. F.; Jarzaba, W. *Adv. Photochem.* **1990**, *1*, 15.
- (3) Simon, J. D. *Acc. Chem. Res.* **1988**, *21*, 21.
- (4) Gustavsson, T.; Cassara, L.; Gulbinas, V.; Gurzadyan, G.; Mialocq, J.-C.; Pommeret, S.; Sorgius, M.; van der Meulen, P. *J. Phys. Chem. A* **1998**, *102*, 4229.
- (5) Bagchi, B.; Chandra, A. *Adv. Chem. Phys.* **1991**, *1*, 80. Bagchi, B. *Annu. Rev. Phys. Chem.* **1989**, *115*, 40.
- (6) Ladanyi, B.; Skaf, M. S. *Annu. Rev. Phys. Chem.* **1993**, *335*, 44.
- (7) Rosental, S. J.; Xie, X.; Du, M.; Fleming, G. R. *J. Chem. Phys.* **1991**, *95*, 4715.
- (8) Jarzaba, W.; Walker, G. W.; Johnson, A. E.; Barbara, P. F. *Chem. Phys.* **1991**, *152*, 57.
- (9) Gardecki, J.; Maroncelli, M. *Chem. Phys. Lett.* **1999**, *301*, 571.
- (10) Suppan, P. *J. Chem. Soc., Faraday Trans. 1* **1987**, *83*, 495.
- (11) Suppan, P. *Photochem. Photobiol. A: Chemistry* **1990**, *50*, 293.
- (12) Suppan, P. *J. Chem. Soc., Faraday Trans.* **1992**, *88*, 963.
- (13) Lurf, C.; Suppan, P. *Chem. Soc. Faraday Trans.* **1992**, *87*, 963.

- (14) Zurawsky, W.; Scarlata, S. *J. Phys. Chem.* **1992**, *96*, 6012.
(15) Zurawsky, W.; Scarlata, S. *Photochem. Photobiol.* **1994**, *60*, 343.
(16) Khajehpour, M.; Kauffman, J. F. *J. Phys. Chem. A* **2000**, *104*, 7151.
(17) Khajehpour, M.; Welch, C. M.; Kleiner, K. A.; Kauffman, J. F. *J. Phys. Chem. A* **2001**, *105*, 5372.
(18) Petrov, N. K.; Wiessner, A.; Fiebig, T.; Straerk, H. *Chem. Phys. Lett.* **1995**, *241*, 127.
(19) Petrov, N. K.; Wiessner, A.; Straerk, H. *J. Chem. Phys.* **1998**, *108*, 2326.
(20) Cichos, F.; Willert, A.; Rempel, U.; von Borczyskowski, C. *J. Phys. Chem. A* **1997**, *101*, 8179.
(21) Cichos, F.; Brown, R.; Rempel, U.; von Borczyskowski, C. *J. Phys. Chem. A* **1999**, *103*, 2506.
(22) Luther, B. M.; Kimmel, J. R.; Levinger, N. E. *J. Chem. Phys.* **2002**, *116*, 3370.
(23) Agmon, N. *J. Phys. Chem. A* **2002**, *106*, 7256.
(24) Molotsky, T.; Huppert, D. *J. Phys. Chem. A* **2002**, *106*, 8525.
(25) Chandra, A.; Bagchi, B. *J. Chem. Phys.* **1991**, *94* (12), 8367.
(26) Raju, B. B.; Costa, S. M. B. *Phys. Chem. Chem. Phys.* **1999**, *1*, 3539.
(27) Krolicki, R.; Jarzeba, W.; Mostafavi, M.; Lampre, I. *J. Phys. Chem. A* **2002**, *106*, 1708.
(28) Molotsky, T.; Huppert, D. *J. Phys. Chem.* **2003**, *107*, 2769.
(29) Marcus, Y. *Solvent Mixtures. Properties and Selective Solvation*; Marcel Dekker: New York, Basel, 2002.
(30) Belletête, M.; Lessard, G.; Durocher, G. *J. Luminescence* **1989**, *42*, 337.
(31) Andrade, S. M.; Costa, S. M. B. *Phys. Chem. Chem. Phys.* **1999**, *1*, 4213.
(32) Day, T. J. F.; Patey, G. N. *J. Chem. Phys.* **1999**, *110*, 10937.
(33) Nishiyama, K.; Okada, T. *J. Phys. Chem. A* **1998**, *102*, 9729.
(34) Ladanyi, B. M.; Perng, B.-C. *J. Phys. Chem. A* **2002**, *106*, 6922.
(35) Lind, J. E.; Fuoss, R. M. *J. Phys. Chem.* **1961**, *65*, 999.
(36) Reynolds, L.; Gardecki, J. A.; Franland, S. J. V.; Horng, M. L.; Maroncelli, M. *J. Phys. Chem.* **1996**, *100*, 10337.
(37) Laurence, C.; Nicolet, P.; Dalati, M. T.; Abboud, J.-L. M.; Notario, R. *J. Phys. Chem.* **1994**, *98*, 5807.
(38) Kamlet, M. J.; Abboud, J.-L. M.; Abraham, M. H.; Taft, R. W. *J. Org. Chem.* **1983**, *48*, 2877.
(39) Reichardt, C. *Solvents and Solvent Effects in Organic Chemistry*; VCH: Weinheim, 1979.
(40) Chapman, C. F.; Maroncelli, M. *J. Phys. Chem.* **1991**, *95*, 9095.
(41) Argaman, R.; Huppert, D. *J. Phys. Chem. B* **2000**, *104*, 1338.
(42) Argaman, R.; Molotsky, T.; Huppert, D. *J. Phys. Chem. A* **2000**, *104*, 7934.
(43) Errera, J.; Gaspard, R.; Sack, H. *J. Chem. Phys.* **1940**, *8*, 63.
(44) Gordy, W. *J. Chem. Phys.* **1936**, *4*, 769.
(45) Fratiello, A.; Douglass, D. C. *J. Mol. Spectrosc.* **1963**, *11*, 465.
(46) Fauconnier, C.; Harrand, M. *Ann. Phys.* **1956**, *1*, 5.
(47) Clemett, C. J.; Forest, E.; Smyth, C. P. *J. Chem. Phys.* **1964**, *40*, 2123.
(48) Wu, Y. G.; Tabata, M.; Takamuku, T. *J. Mol. Liq.* **2001**, *94*, 273.
(49) Yoshida, K.; Yamaguchi, T.; Nagao, M. *Appl. Phys. A Mater. Sci. Processing* **2002**, *74*, S386.